

Pressure Induced Stripe-order Antiferromagnetism and First-order Phase Transition in FeSe

P. S. Wang,¹ S. S. Sun,¹ Y. Cui,¹ W. H. Song,¹ T. R. Li,¹ Rong Yu,^{1,2,*} Hechang Lei,^{1,†} and Weiqiang Yu^{1,2,‡}

¹*Department of Physics and Beijing Key Laboratory of Opto-electronic Functional Materials & Micro-nano Devices, Renmin University of China, Beijing, 100872, China*

²*Department of Physics and Astronomy, Shanghai Jiao Tong University, Shanghai 200240, China and Collaborative Innovation Center of Advanced Microstructures, Nanjing 210093, China*

(Dated: May 27, 2022)

To elucidate the magnetic structure and the origin of the nematicity in FeSe, we perform a high-pressure ⁷⁷Se NMR study on FeSe single crystals. We find a suppression of the structural transition temperature with pressure up to about 2 GPa from the anisotropy of the Knight shift. Above 2 GPa, a stripe-order antiferromagnetism that breaks the spatial four-fold rotational symmetry is determined by the NMR spectra under different field orientations and with temperatures down to 50 mK. The magnetic phase transition is revealed to be first-order type, implying the existence of a concomitant structural transition via a spin-lattice coupling. Stripe-type spin fluctuations are observed at high temperatures, and remain strong with pressure. These results provide clear evidences for strong coupling between nematicity and magnetism in FeSe, and therefore support a universal scenario of magnetic driven nematicity in iron-based superconductors.

PACS numbers: 74.70.-b, 76.60.-k

In most iron-based superconductors, superconductivity emerges near an antiferromagnetic (AFM) phase, making it important to study the nature of their magnetism [1–3]. For iron pnictides, the magnetic ground state typically has a stripe-type, or $(\pi, 0)$, AFM order [4]. The magnetic transition at T_N is preceded by a tetragonal-to-orthorhombic structural transition at $T_s \geq T_N$ where the lattice C_4 symmetry is broken, and the orthorhombic phase is denoted as a nematic state. The nematicity can be observed as anisotropy in the in-plane resistivity [5] and spin fluctuations [4], and the splitting of the degenerate d_{xz}/d_{yz} orbitals [6] (so called orbital ordering [7]). Although it is generally believed that the nematicity has an electronic origin, it is still highly debated whether the nematicity is driven by the spin fluctuations or the orbital ordering [8].

Recent discoveries in the bulk FeSe superconductors [9] make this unsolved issue even more elusive: at ambient pressure, the electronic nematicity shows up below $T_s \sim 90$ K [10, 11], while a magnetic ordered state is absent. Applying pressure above 1 GPa, however, magnetic ordering emerges, and the ordering temperature T_N increases with pressure [12, 13]. Meanwhile, T_s is substantially suppressed at ~ 2 GPa [14, 15]. These seemingly sharp contrasts between FeSe and iron pnictides challenge the existed view of the interplay among nematicity, orbital ordering and magnetism, and inspire various theoretical proposals for the nature of magnetism in FeSe [16–19]. On the experimental side, inelastic neutron scattering measurements suggest the coexistence of stripe and checkerboard spin fluctuations at ambient pressure [20, 21], and transport measurements report high-temperature superconductivity (HTSC) in both the ambient-pressure nematic and the high-pressure mag-

netic phases [14, 15, 22, 23]. Therefore, resolving the nematicity and the magnetic structure in FeSe not only helps building up the proper theory on the magnetism of FeSe, but also becomes important in understanding the HTSC in FeSe and other iron-based superconductors.

In this work, we present our ⁷⁷Se NMR studies on high-quality FeSe single crystals with pressures up to 2.4 GPa and temperatures down to 50 mK. Our main results are summarized in the phase diagram of Fig. 1. From the pressure dependence of the NMR spectral splitting under an in-plane magnetic field, we observe a decrease of the structural transition temperature T_s with pressure. However, the stripe-type spin fluctuations, characterized by the anisotropic $1/^{77}T_1T$, are enhanced below a weakly pressure dependent temperature $T^* \sim 100$ K. We find that the magnetic ordering emerges about ~ 0.2 GPa higher than earlier reports [14, 15]. The magnetic transition at T_N above 2 GPa is first-order, and T_N increases with pressure. The S-AFM phase necessarily breaks the C_4 symmetry as the magnetic ordering in iron pnictides. The discovery of the strong stripe-type spin fluctuations at high temperatures, the first-order magnetic transition, and the low-temperature S-AFM ground state under pressure clearly reveals a universal magnetic origin of the nematicity in both FeSe and iron pnictides. They also shed light on the important role of magnetism on superconductivity in iron-based superconductors.

Details of FeSe single crystal synthesis and characterization are presented in supplemental S1 and S2. The superconducting transition temperature T_c is determined *in situ* by the RF inductance of the NMR coil (supplemental S3). The NMR measurements were performed under 10.3 T with two field configurations, $H \parallel a&b$ (tetragonal [1 1 0] direction) and $H \parallel c$. Daphne oil was used as the

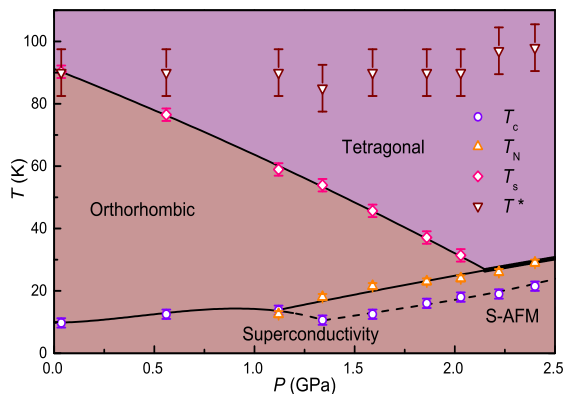


FIG. 1: (color online). The (P, T) phase diagram with T_s , T_N , T_c , and T^* (see text for definition). The S-AFM phase is observed below T_N above 2 GPa. The first-order magnetic transition is indicated by the bold solid line of T_N . The solid line connecting the T_c points presents superconductivity observed in both the RF inductance and the $1/T_1$, and the dashed line presents superconductivity only seen in the RF inductance.

pressure medium, and the pressure was determined by Cu_2O NQR resonant frequency at 5 K [24]. For applying pressure above 2 GPa, the cell was heated to 80 °C in order to improve pressure hydrostaticity [25]. Standard spin-echo and CPMG techniques were used for data accumulation to optimize the signal-to-noise ratio. The full-width-of-half-maximum (FWHM) of ^{77}Se spectra is ~ 3 kHz at 300 K at all pressures, indicating high sample quality and pressure homogeneity. The spin-lattice relaxation rates were measured with the inversion-recovery method, where perfect single-exponential functions with time are found with no signal loss or wipeout effect above T_N .

We first determine the evolution of the structural transition under pressure by tracing the NMR line splitting with $H \parallel a\&b$ [26, 27]. In the orthorhombic phase, the in-plane Knight shift is anisotropic. This leads to two resonance peaks respectively corresponding to $H \parallel a$ and $H \parallel b$ due to structural twinning. In Fig. 2(a), NMR spectra are shown at $P = 0.56$ GPa for several selected temperatures, with evidence of structural transition from the NMR line splitting below T_s . The difference of Knight shifts, $\Delta^{77}K_{a,b} = |^{77}K_a - ^{77}K_b|$, where $^{77}K_a$ and $^{77}K_b$ are the Knight shifts for $H \parallel a$ and $H \parallel b$ respectively, follows a mean-field like temperature dependence, consistent with a second-order phase transition [26]. Similar behavior of $\Delta^{77}K_{a,b}$ is observed with pressures up to ~ 2 GPa (Fig. 2(b)). As presented in the phase diagram (Fig. 1), T_s shows a gradual suppression with pressure below 2 GPa. At $P = 2.4$ GPa, line splitting is absent above T_N and cannot be resolved below T_N (Fig. 3(a)).

Next we study the magnetic ordering in the pressurized

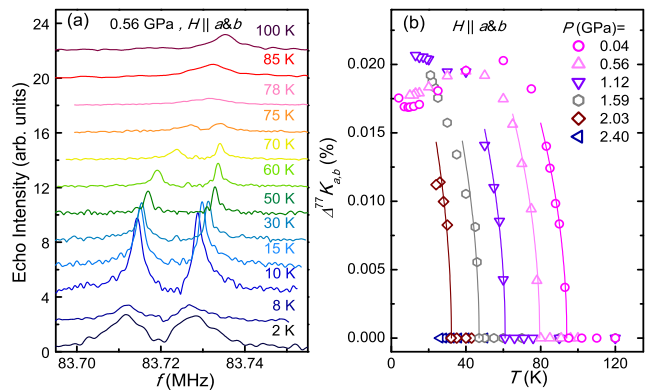


FIG. 2: (color online). (a) The characteristic ^{77}Se spectra showing the structure transition by the line splitting with $H \parallel a\&b$ at $P = 0.56$ GPa. (b) The difference of Knight shifts, $\Delta^{77}K_{a,b} = |^{77}K_a - ^{77}K_b|$, measured as functions of temperature at various pressures. The solid lines are fits to mean-field functions $\Delta^{77}K_{a,b} \sim 1/(T_s - T)^{1/2}$.

phase. Below T_s , the spin-lattice relaxation rates, $1/^{77}T_1$, are different for two frequency peaks with $H \parallel a\&b$, and data are presented in Fig. 4(a)-(c) for the high-frequency peak and Fig. S5 for both peaks for comparison. The $1/^{77}T_1$ is larger for the high-frequency peak (Fig. S5), and the data for two frequencies at low pressures are consistent with the earlier report [26]. For $P > 1.34$ GPa, a magnetic phase transition is clearly seen from the peaked feature in $1/^{77}T_1T$ (Fig. 4(b)-(c) and S5) and the broadening of the NMR spectra upon cooling. Typical spectral data at 2.4 GPa are shown in Fig. 3(a)-(c). Below 30 K, the spectrum with $H \parallel a\&b$ shifts slightly to the high-frequency side, and its FWHM increases from ~ 10 kHz at $T = 30$ K to ~ 300 kHz at $T = 26$ K (Fig. 3(a)), signaling the magnetic transition. Upon cooling, the spin-spin relaxation time $^{77}T_2$ increases from ~ 5 ms at 120 K to ~ 20 ms below T_N , which ensures correct analysis on the spectral weight. In Fig. 3(c), the normalized total spectral weight is drawn as a function of temperature at this pressure. The weight drops steeply by 50% from $T = 30$ K to 26 K across the magnetic transition, develops a plateau-like feature between 26 K and 18 K, and then decreases slowly upon further cooling due to RF screening below T_C .

The $1/^{77}T_1$ shows a sudden drop at 28 K defined as T_N , coinciding with the middle point of the magnetic transition from the spectral loss. With $H \parallel c$, the spectra keep narrow (Fig. 3(b)), but the total spectral weight decreases when cooled below 30 K and reaches zero at 26 K (Fig. 3(c)). Two split broad NMR lines (~ 300 kHz) are seen at 50 mK (Fig. 3(b)), corresponding to $H_{in}^c \approx \pm 0.48$ T.

The split spectra with $H \parallel c$ and the large spectral weight with $H \parallel a\&b$ resemble the ^{75}As NMR spectra of stripe ordering in the iron pnictides [28]. By applying

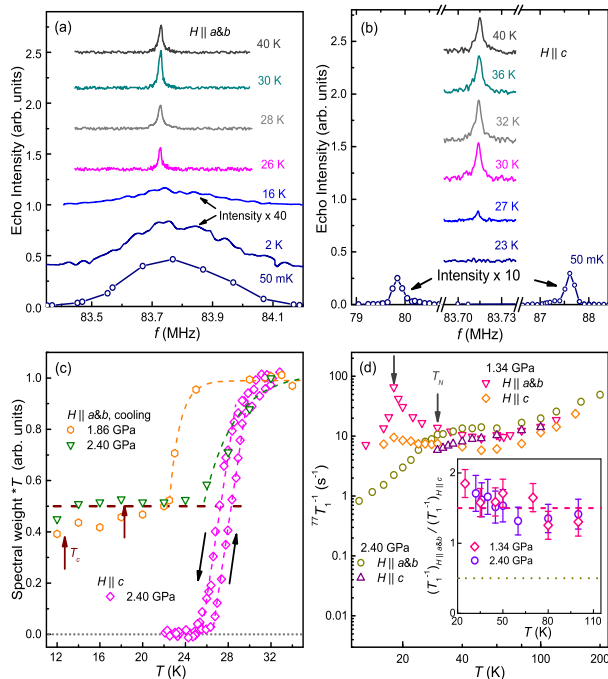


FIG. 3: (color online). (a) and (b): The NMR spectra with $H \parallel a\&b$ and $H \parallel c$ at $P = 2.4$ GPa. (c) The normalized total spectral weight as a function of temperature at high pressures. T_c are determined by the RF inductance under the same field. (d) The $1/^{77}T_1$ for $H \parallel a\&b$ (averaged for two frequency peaks below T_s) and $H \parallel c$, at $P = 1.34$ and 2.4 GPa. Inset: the anisotropy factor $R = (1/^{77}T_1)_{H \parallel a\&b} / (1/^{77}T_1)_{H \parallel c}$ as a function of temperature. The dashed and dotted horizontal lines are the theoretical values for the stripe-type ($R = 1.5$) and for the checkerboard-type ($R = 0.5$) spin fluctuations.

the same analysis on ^{77}Se [28, 29](supplemental S4), we show that the change of the spectral weight below T_N is caused by the formation of a stripe-type AFM order. The ordered moment on Fe sites is projected as $(m_{Fe}^a, m_{Fe}^b, m_{Fe}^c)$ to the principal axes of the orthorhombic structure, and the hyperfine field on the ^{77}Se is calculated to be $(H_{in}^a, H_{in}^b, H_{in}^c) = A_{hf}^{ac}(m_{Fe}^c, 0, m_{Fe}^a)$, where A_{hf}^{ac} is an off-diagonal hyperfine coupling constant. With a finite $\pm m_{Fe}^a$ ($\pm H_{in}^a$), the spectrum splits for $H \parallel c$ but does not split for $H \parallel b$. This produces exactly what we have observed in the ordered phase: with $H \parallel c$ only symmetric NMR lines are observed ~ 3.9 MHz away from the center, whereas with $H \parallel b$ spectral weight remains near the paramagnetic frequency.

The disappearance of the paramagnetic peak with $H \parallel c$ indicates that the sample is fully magnetically ordered. The 50% signal loss with $H \parallel a\&b$ could be caused by a broad spectrum from distributed magnetic moments, or a very short T_2 from phase inhomogeneity. Moreover, we find that the signal loss remains 50% for different pressures and samples, and another plausible explanation is that one of the two domains is out of the NMR window in the stripe phase. In particular, if m_{Fe}^c

(H_{in}^a) is finite, the signal is lost for $H \parallel a$ but not for $H \parallel b$. However, further experimental evidences and theoretical understanding are requested to fully settle this scenario.

The above analyses already allow us to rule out other proposed local patterns, such as the checkerboard (π, π) spin orders where a zero c -axis internal field is expected on the Se sites (supplemental S4). In fact, it has been suggested theoretically that the lack of magnetic ordering at the ambient pressure is caused by competing interactions, such as strong magnetic frustration from nearest and next nearest neighbor exchange couplings J_1 and J_2 [16–19]. Our observation under pressure puts strong constraints on these competing theories: naively, our finding of the S-AFM phase suggests a reduced ratio of J_1/J_2 with pressure. This is also consistent with an *ab initio* DFT calculation, where the S-AFM state has the lowest energy over other magnetic states under pressure [18].

This high-pressure magnetic order of FeSe naturally resembles that of the iron pnictides [4], and therefore may fit to a unified magnetic phase diagram of the iron-based superconductors generated by the competing exchange interactions. The stripe order with a finite m_{Fe}^a clearly indicates a magnetic C_4 symmetry breaking because of two choices to select a -axis of the crystals. Furthermore, a strong spin-lattice coupling has to be considered in the magnetic phase transition as shown below. We examined the magnetic transition across T_N from the temperature scan of the $1/^{77}T_1T$, as shown in Fig. 4(a)-(c) for the high-frequency peak. In fact, the following discussions are valid for the low-frequency peak as well (see Fig. S5). For pressures from 1.34 GPa to 1.86 GPa, the $1/^{77}T_1T$ has a clear divergence at T_N , suggesting a second-order magnetic transition. Surprisingly, the divergence is completely absent at T_N under higher pressures (≥ 2 GPa), directly evidencing a strong first-order transition with no critical fluctuations. The first-order nature of the transition is further supported by the hysteresis near T_N , with a 1.5 K shift in the temperature dependence of the integrated spectral weight with $H \parallel c$ between cooling and warming at 0.1 K/minute (Fig. 3(c)). This strongly implies that the magnetic transition is coupled to a tetragonal-to-orthorhombic structural transition due to the strong spin-lattice coupling [30, 31]. The simultaneous magnetic and structural transition are also supported by the high-pressure XRD data [32, 33]. It also suggests that the structural transition is an Ising-nematic transition with a magnetic origin [34, 35].

We are now in a position to discuss the spin fluctuations above T_N from the $1/^{77}T_1$ data. Fig. 3(d) shows the $(1/^{77}T_1)_{H \parallel a\&b}$ and $(1/^{77}T_1)_{H \parallel c}$ below 200 K at $P = 1.34$ GPa and 2.4 GPa. In the inset, the anisotropy factor $R = (1/^{77}T_1)_{H \parallel a\&b} / (1/^{77}T_1)_{H \parallel c}$ at these two pressures are presented, where $R \approx 1.5$ holds from 100 K down to 40 K. This value of R is an indication of stripe-type, or $(\pi, 0)$, spin fluctuations at temperatures far

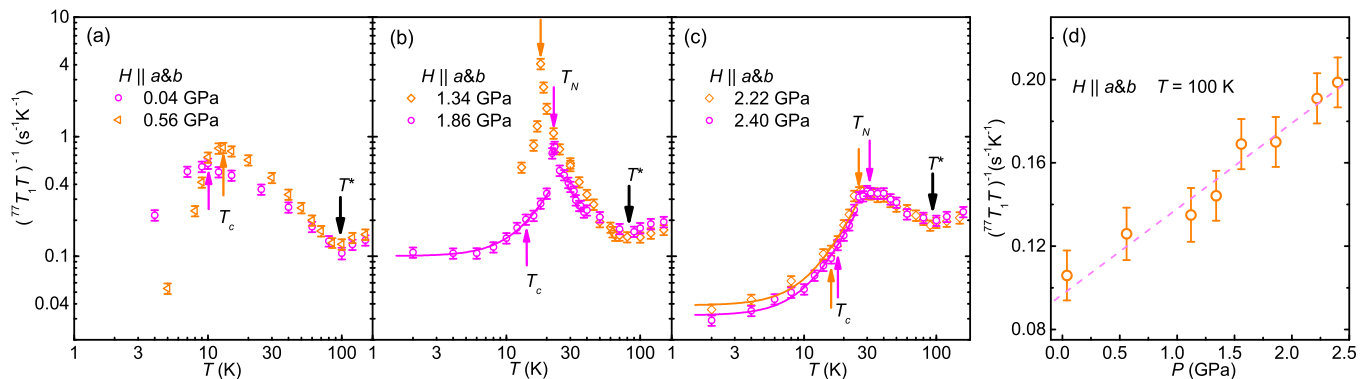


FIG. 4: (color online). (a), (b), (c): The spin-lattice relaxation rate divided by temperature ($1/^{77}T_1T$) with $H \parallel a\&b$ at typical pressures. Only the data measured on the high-frequency peaks are presented below T_s . The T_c (determined by RF inductance under the same field), the T_N , and the T^* are marked by the arrows. (d) The plot of $1/^{77}T_1T$ at 100 K as a function of pressure.

above T_N (supplemental S4). $R \approx 1.5$ persists to the highest pressure we measured, and is consistent with the ground state magnetism we presented. The possibility of checkerboard-type spin fluctuations [21] with $R \approx 0.5$ (see Fig. 3(d) inset) is ruled out at high pressures.

Remarkably, as shown in Fig. 4(a)-(c), the high-temperature $1/^{77}T_1T$ first decreases upon cooling below 200 K, and then shows an upturn behavior with further decrease of temperature. For each pressure, we define a characteristic temperature T^* for the onset of the upturn [as shown in Fig. 4(a)-(c)], which indicates enhanced low-energy spin fluctuations. The T^* barely varies with pressure within our resolution, as shown in the phase diagram (Fig. 1). The error bars of T^* are taken as distances between two temperatures where $1/^{77}T_1T$ is enhanced by 10% when cooling/warming away from T^* . Furthermore, the $1/^{77}T_1T$ at 100 K, as presented in Fig. 4(d), also increases with pressure, consistent with earlier NMR results on polycrystals [12]. Therefore, our high-pressure data reconcile FeSe and other iron-based superconductors, where the stripe order and the $(\pi, 0)$ fluctuations tend to be universal, although distinct properties are observed in FeSe at the ambient pressure.

These high-pressure data shed important new light on the driving force of the nematicity. First, in the full range of pressure we have measured, enhanced low-energy stripe-type spin fluctuations exist up to T^* . T^* only accidentally coincides with T_s (orbital ordering) at $P = 0$, but surpasses T_s largely at high pressures. The emergence of high-temperature stripe-type spin fluctuations is hardly understood within an orbital-driven-nematicity scenario [26], but could be explained as enhanced spin fluctuations above the Ising-nematic transition in a magnetic-driven-nematicity scenario [36]. Second, the concomitant structural transition above 2 GPa, manifest by the first-order magnetic phase transition, evidences a strong coupling between nematicity and magnetism under pressure. This scenario implies

the same underlying physics governing the coupled magnetic and nematic transitions in some iron pnictides [37], and hence suggests a universal picture of a magnetic-driven nematicity in iron-based superconductors [8]. Furthermore, it has been proposed that frustrated magnetic exchange interactions at low pressures may favor other magnetic orders, such as the antiferroquadrupolar order [16] and/or the staggered dimmer/trimmer order [18, 19]. These exotic magnetic states support the same nematic order, but compete with the stripe-order magnetism. With increasing pressure, these competing orders may be suppressed while the stripe correlations grow strongly, which lead to a non-monotonic change of T_s [16, 18] as we observed.

Finally, we address the implications of our data to superconductivity. Besides the RF inductance measurements (supplemental S3), the onset of superconductivity below 1 GPa is also shown by a kinked feature in the $1/^{77}T_1T$ upon cooling (Fig. 4(a)), which signals bulk superconductivity. Above 1.5 GPa, while both T_c and T_N increase with pressures, the $1/^{77}T_1T$ drops smoothly and fits to $1/^{77}T_1T = a + bT^\alpha$ with $\alpha \approx 2.5$ (presented by the solid lines in Fig. 4(b-c)), which is a typical form by taking into account the contributions from both itinerant electrons and spin waves far below T_N . The absence of a kinked feature across T_c in $1/^{77}T_1T$ excludes the microscopic coexistence of superconductivity in our observed stripe phase. However, further investigation is needed to address the exact locations and the properties of the superconducting phase. Since superconductivity does not show up in the observed magnetic regions, we speculate that it exists in small inhomogeneous or short T_2 regions as we described earlier. Nevertheless, the proximity of the superconducting phase to the stripe order and existence of strong $(\pi, 0)$ spin fluctuations in the paramagnetic phase, draw a close relation between superconductivity and the stripe-order magnetism, as seen in iron pnictides. Future studies under higher pressures, when

magnetic ordering is suppressed [15], may shed further light on the pairing mechanism [38, 39].

In summary, we report direct spectroscopic evidence for the strong suppression of the orbital ordering/structure transition under pressure, and for a stripe-order magnetism above 2 GPa in FeSe. The magnetic transition is identified as a first-order type with a C_4 symmetry breaking. These pressure effects put constraints on theories of magnetism in FeSe. Although the T_S is not directly detected by the current NMR data above 2 GPa, electronic nematicity and nematic fluctuations are shown to be closely coupled to the stripe-order magnetism, resulting in a first-order magnetic and structural transition under high pressures and persistent strong (π , 0) spin fluctuations over a wide range of temperature and pressure. These results suggest a strong coupling among lattice, magnetism, and nematicity, and fully support a magnetic-driven-nematicity scenario. Our high-pressure data also reconcile FeSe with other iron-based superconductors by the stripe-order magnetism, and helps to understand the superconductivity on a universal basis.

We acknowledge encouraging discussions with Zhong-Yi Lu, Dong-Hai Lee, Tao Xiang, Kai Liu, Fa Wang, and Qimiao Si. Work at Renmin University of China is supported by the National Science Foundation of China (NSFC) (Grant Nos. 11222433, 11374361, 11374364 and 11574394), the Ministry of Science and Technology of China (Grant Nos. 2016YFA0300504), and the Fundamental Research Funds for the Central Universities and the Research Funds of Renmin University of China (Grant Nos. 14XNLF08, 15XNLF07 and 15XNLF06).

* Electronic address: rong.yu@ruc.edu.cn

† Electronic address: hlei@ruc.edu.cn

‡ Electronic address: wqyu@phy@ruc.edu.cn

- [1] J. Paglione, and R. L. Greene, *Nature Phys.* **6**, 645 (2010).
- [2] G. R. Stewart, *Rev. Mod. Phys.* **83**, 1589 (2011).
- [3] P. Dai, *Rev. Mod. Phys.* **87**, 855 (2015).
- [4] C. de la Cruz, Q. Huang, J. W. Lynn, J. Li, W. Ratcliff II, J. L. Zarestky, H. A. Mook, G. F. Chen, J. L. Luo, N. L. Wang, and P. Dai, *Nature* **453**, 899 (2008).
- [5] J.-H. Chu, J. G. Analytis, K. De Greve, P. L. McMahon, Z. Islam, Y. Yamamoto and I. R. Fisher, *Science* **329**, 824 (2010).
- [6] M. Yi, D. Lu, J.-H. Chu, J. G. Analytis, A. P. Sorini, A. F. Kemper, B. Moritz, S.-K. Mo, R. G. Moore, M. Hashimoto, W.-S. Lee, Z. Hussain, T. P. Devereaux, I. R. Fisher, and Z.-X. Shen, *Proc. Natl. Acad. Sci.* **108**, 6878 (2011).
- [7] W. Lv, F. Krüger, and P. Phillips, *Phys. Rev. B* **82**, 045125 (2010).
- [8] R. M. Fernandes, A. V. Chubukov, and J. Schmalian, *Nature Phys.* **10**, 97 (2014).
- [9] F.-C. Hsu, J.-Y. Luo, K.-W. Yeh, T.-K. Chen, T.-W. Huang, P. M. Wu, Y.-C. Lee, Y.-L. Huang, Y.-Y. Chu, D.-C. Yan, and M.-K. Wu, *Proc. Natl. Acad. Sci.* **105**, 14262 (2008).
- [10] T. M. McQueen, A. J. Williams, P. W. Stephens, J. Tao, Y. Zhu, V. Ksenofontov, F. Casper, C. Felser, and R. J. Cava, *Phys. Rev. Lett.* **103**, 057002 (2009).
- [11] T. Shimojima, Y. Suzuki, T. Sonobe, A. Nakamura, M. Sakano, J. Omachi, K. Yoshioka, M. Kuwata-Gonokami, K. Ono, H. Kumigashira, A. E. Böhmer, F. Hardy, T. Wolf, C. Meingast, H. v. Löhneysen, H. Ikeda, and K. Ishizaka, *Phys. Rev. B* **90**, 121111(R) (2014).
- [12] T. Imai, K. Ahilan, F. L. Ning, T. M. McQueen, and R. J. Cava, *Phys. Rev. Lett.* **102**, 177005 (2009).
- [13] M. Bendele, A. Amato, K. Conder, M. Elender, H. Keller, H.-H. Klauss, H. Luetkens, E. Pomjakushina, A. Raselli, and R. Khasanov, *Phys. Rev. Lett.* **104**, 087003 (2010).
- [14] T. Terashima, N. Kikugawa, S. Kasahara, T. Watashige, T. Shibauchi, Y. Matsuda, T. Wolf, Anna E. Böhmer, Frédéric Hardy, C. Meingast, H. v. Löhneysen, and S. Uji, *J. Phys. Soc. Jpn.* **84**, 063701 (2015).
- [15] J. P. Sun, K. Matsuura, G. Z. Ye, Y. Mizukami, M. Shimozawa, K. Matsubayashi, M. Yamashita, T. Watashige, S. Kasahara, Y. Matsuda, J.-Q. Yan, B. C. Sales, Y. Uwatoko, J.-G. Cheng, and T. Shibauchi, *Nat. Commun.* **7**, 12146 (2016).
- [16] R. Yu and Q. Si, *Phys. Rev. Lett.* **115**, 116401 (2015).
- [17] F. Wang, S. A. Kivelson, and D.-H. Lee, *Nature Phys.* **11**, 959 (2015).
- [18] J. K. Glasbrenner, I. I. Mazin, Harald O. Jeschke, P. J. Hirschfeld, R. M. Fernandes, and Roser Valentí, *Nature Phys.* **11**, 953 (2015).
- [19] K. Liu, Z.-Y. Lu, and T. Xiang, *Phys. Rev. B* **93**, 205154 (2016).
- [20] M. C. Rahn, R. A. Ewings, S. J. Sedlmaier, S. J. Clarke, and A. T. Boothroyd, *Phys. Rev. B* **91**, 180501(R) (2015).
- [21] Q. Wang, Y. Shen, B. Pan, X. Zhang, K. Ikeuchi, K. Iida, A. D. Christianson, H. C. Walker, D. T. Adroja, M. Abdel-Hafez, Xiaojia Chen, D. A. Chareev, A. N. Vasiliev, and J. Zhao, *Nat. Commun.* **7**, 12182 (2016).
- [22] G. Garbarino, A. Sow, P. Lejay, A. Sulpice, P. Toulemonde, M. Mezouar, and M. Núñez-Regueiro, *Europhys. Lett.* **86**, 27001 (2009).
- [23] S. Medvedev, T. M. McQueen, I. A. Troyan, T. Palasyuk, M. I. Eremets, R. J. Cava, S. Naghavi, F. Casper, V. Ksenofontov, G. Wortmann, and C. Felser, *Nature Mater.* **8**, 630 (2009).
- [24] A. P. Reyes, E. T. Ahrens, R. H. Heffner, P. C. Hammel, and J. D. Thompson, *Rev. Sci. Instrum.* **63**, 3120 (1992).
- [25] K. Yokogawa, K. Murata, H. Yoshino, and S. Aoyama, *Jpn. J. Appl. Phys.* **46**, 2626 (2007).
- [26] S.-H. Baek, D. V. Efremov, J. M. Ok, J. S. Kim, Jeroen van den Brink, and B. Büchner, *Nature Mater.* **14**, 210 (2015).
- [27] A. E. Böhmer, T. Arai, F. Hardy, T. Hattori, T. Iye, T. Wolf, H. v. Löhneysen, K. Ishida, and C. Meingast, *Phys. Rev. Lett.* **114**, 027001 (2015).
- [28] K. Kitagawa, N. Katayama, K. Ohgushi, M. Yoshida, and M. Takigawa, *J. Phys. Soc. Jpn.* **77**, 114709 (2008).
- [29] S. Kitagawa, Y. Nakai, T. Iye, K. Ishida, Y. Kamihara, M. Hirano, and H. Hosono, *Phys. Rev. B* **81**, 212502 (2010).
- [30] Q. Q. Ye, K. Liu, and Z. Y. Lu, *Phys. Rev. B* **88**, 205130 (2013).
- [31] J. Lischner, T. Bazhiron, A. H. MacDonald, M. L. Cohen, and S. G. Louie, *Phys. Rev. B* **91**, 020502(R) (2015).

- [32] S. Margadonna, Y. Takabayashi, Y. Ohishi, Y. Mizuguchi, Y. Takano, T. Kagayama, T. Nakagawa, M. Takata, and K. Prassides, *Phys. Rev. B* **80**, 064506 (2009).
- [33] K. Kothapalli, A. E. Böhmer, W. T. Jayasekara, B. G. Ueland, P. Das, A. Sapkota, V. Taufour, Y. Xiao, E. Alp, S. L. Bud'ko, P. C. Canfield, A. Kreyssig, and A. I. Goldman, *Nat. Comm.* **1**, 12728 (2016).
- [34] C. Fang, H. Yao, W.-F. Tsai, J. P. Hu, and S. A. Kivelson, *Phys. Rev. B* **77**, 224509 (2008).
- [35] J. Dai, Q. Si, J.-X. Zhu, and E. Abrahams, *Proc. Natl. Acad. Sci.* **106**, 4418 (2009).
- [36] R. Yu, Z. Wang, P. Goswami, A. H. Nevidomskyy, Q. Si, and E. Abrahams, *Phys. Rev. B* **86**, 085148 (2012).
- [37] S. Kasahara, H. J. Shi, K. Hashimoto, S. Tonegawa, Y. Mizukami, T. Shibauchi, K. Sugimoto, T. Fukuda, T. Terashima, Andriy H. Nevidomskyy, and Y. Matsuda, *Nature* **486**, 382 (2012).
- [38] F. Essenberg, A. Sanna, P. Buczek, A. Ernst, L. Sandratskii, and E.K.U. Gross, arXiv:1411.2121.
- [39] T. Watashige, Y. Tsutsumi, T. Hanaguri, Y. Kohsaka, S. Kasahara, A. Furusaki, M. Sigrist, C. Meingast, T. Wolf, H. v. Löhneysen, T. Shibauchi, and Y. Matsuda, *Phys. Rev. X* **5**, 031022 (2015).